Rhizophere analysis of auxin producers harboring the phenylpyruvate decarboxylase pathway

Cécile Gruet, Andréa Oudot, Danis Abrouk, Yvan Moënne-Loccoz, Daniel Muller

Rhizophere analysis of auxin producers harboring the phenylpyruvate decarboxylase pathway

Cécile Gruet, Andréa Oudot, Danis Abrouk, Yvan Moënne-Loccoz, Daniel Muller

Univ Lyon, Université Claude Bernard Lyon 1, CNRS, INRAe, VetAgro Sup, UMR5557 Ecologie Microbienne, 43 bd du 11 novembre 1918, F-69622 Villeurbanne, France

Current address for Andréa Oudot: Université Paris Est Créteil (UPEC), Laboratoire Eau Environnement et Systèmes Urbains (LEESU), 61 avenue Général De Gaulle, F-94010 Créteil, France

Abstract

The 3-indole acetic acid (IAA) produced by microorganisms in the rhizosphere modulates root growth and physiology, but the analysis of these microorganisms relies on the isolation of culturable IAA producers as molecular tools are lacking. Microbial biosynthesis of IAA may involve several pathways, like the phenylpyruvate decarboxylase pathway (using the *ppdC* gene) present in many phytobeneficial microorganisms. Here, we tested the hypothesis that PCR primers could be developed to quantify *ppdC*$^+$ microorganisms and assess *ppdC* allele diversity in the rhizosphere and bulk soil. Effective *ppdC* primers were obtained and validated *in silico* and using individual *ppdC*$^+$ strains. By qPCR, they enabled to evidence high abundance of *ppdC*$^+$ microorganisms in different types of bulk and rhizospheric soils, up to 8 log of *ppdC* copies per g of soil. OTUs obtained with Illumina sequencing of bulk and rhizospheric soil samples clustered in numerous clades encompassing almost all the known *ppdC* diversity in soil environments, and pointing to soil type and plant species as factors potentially shaping *ppdC* allelic diversity. In conclusion, these new primers enabled the first culture-independent analysis of the *ppdC*$^+$ functional group of IAA producers in environmental samples.

Keywords: Plant growth-promoting rhizobacteria; plant-microbe; functional group; Soil microbiology; holobiont

1. Introduction

The plant root-associated microbiota plays significant roles in plant growth, development, and health, by using direct or indirect mechanisms (Vacheron et al., 2013). Several direct mechanisms implicate the synthesis of signal molecules, leading to molecular communication between partners (Bais et al., 2006). Microbial partners can influence the plant hormonal balance by producing compounds that act as phytohormones, such as auxins (Vacheron et al., 2013). Several types of auxins exist (Korasick et al., 2013) and the most abundant is the 3-indole acetic acid (IAA). IAA acts in different plant processes (Ljung, 2013), by influencing seed germination, tissue elongation in aerial and root parts, organ vascularization, and flowering (Overvoorde et al., 2010; Scarpella et al., 2010).

Several IAA synthesis pathways have been described in microorganisms (Spaepen et al., 2007; Zhao, 2014). In addition to a tryptophan-independent pathway, five tryptophan-dependant pathways are documented, including the phenylpyruvate decarboxylase (PPDC) pathway, indole-3-pyruvate decarboxylase (IPDC) pathway, indole-acetamide (IAM) pathway, tryptophan side-chain oxidase (TSO) pathway, tryptamine (TAM) pathway, and the indole-3-acetonitrile (IAN) pathway (Figure A.1; Costacurta and Vanderleyden, 1995; Di et al., 2015; Morffy and Strader, 2020). Thus, microbial production of IAA implicates several different functional groups (*i.e.* sets of microorganisms performing a same elementary function), and together these functional groups form the total community of IAA producers. In addition, each pathway has been described in different types of microorganisms isolated from roots, pointing towards functional redundancy (Oberhänsli et al. 1991; Prinsen et al. 1993; Zimmer et al. 1997; Spaepen et al. 2007; Kochar et al. 2011; Shao et al. 2015; Liu et al. 2019; Zhang et al. 2019).

The PPDC pathway is the principal IAA synthesis pathway in microbial isolates with phytobeneficial potential (Spaepen et al., 2007; Patten et al., 2012; Mashiguchi et al., 2019). Briefly, tryptophan is transaminated by an aminotransferase into indole-3-pyruvate (Scarpella et al., 2010), which is decarboxylated to form indole-3-acetaldehyde, subsequently oxidized to IAA. Decarboxylation is achieved by indole-3-pyruvate decarboxylases encoded by the *ipdC* or the *ppdC* gene. The two indole-3-

pyruvate decarboxylases do not use the same range of substrates (Schütz et al., 2003). PpdC preferentially uses phenylpyruvate, 5-phenyl-2-oxopentanoate or indole-3-pyruvate, while IpdC uses indole-3-pyruvate or benzoylformate. A phylogenetic study showed that *ipdC* appeared in the last common ancestor of *Pantoea* and *Erwinia,* two genera including several phytopathogens, while *ppdC* appeared in the last common ancestor of *Azospirillum* and *Bradyrhizobium*, i.e. genera well known for their phytobeneficial effects (Bruto et al., 2014). In *Azospirillum baldaniorum* (previously *A. brasilense*) Sp245, known for its plant-beneficial properties, IAA synthesis relies mainly on the PPDC pathway (Spaepen et al., 2007), as a *ppdC*-knockout mutant produced only 10% of wild-type IAA level. The IAM pathway is found, as for the IPDC pathway, in plant-pathogenic strains such as those from species *Dickeya dadantii* (Kunkel and Harper, 2018).

In light of the ecological importance of IAA production by bacteria, it is important to document the microorganisms involved and their functioning. Thus, many studies have focused on isolation of IAA-producing soil bacteria and analysis of auxin production by bacterial isolates (Ali et al., 2009; Bulgarelli et al. 2013; Khalid et al., 2004; Roesch et al., 2007; Spaepen et al 2007; Tsavkelova et al., 2005). However, our knowledge of IAA producers is restricted by the lack of molecular tools, and therefore the diversity and functioning of the IAA-producing community in the rhizosphere remain poorly documented.

The objective of this work was to test the hypothesis that molecular tools could be developed to enable rhizosphere monitoring of the functional group of IAA producers harboring the PPDC pathway, the main IAA pathway documented in phytobeneficial IAA producers. To this end, we used the *ppdC* gene sequence of *Azospirillum brasilense* M1 to recover putative *ppdC* homologues and document the allelic diversity available in bacterial isolates. We developed a primer pair to target the *ppdC* functional group, and assessed its usefulness to monitor the abundance and diversity of *ppdC*$^{+}$ bacteria in bulk and rhizospheric soils.

2. Materials and methods

2.1. Developments of *ppdC* primers

The *ppdC* gene sequence of *Azospirillum brasilense* strain M-1 [accession number KM972378.1] (Jijón-Moreno et al., 2015; Spaepen et al., 2007) was used to search the NCBI database by nucleotide BLAST to recover putative *ppdC* homologues. Only sequences with minimum of 80 % coverage and 40% identity were kept (Oberhänsli et al. 1991). A BLAST using deduced protein sequences was then done with the same parameters. The 44 sequences obtained (each from a different strain) were aligned with Seaview (Gouy et al., 2010) using the Muscle algorithm (Edgar, 2004). A phylogenetic tree was inferred in Seaview with the Neighbor-Joining method, using the Kimura two-parameter method for distance calculation (Figure A.2) (Kimura, 1980). Nodal robustness of the tree was assessed using 1000 bootstrap replicates. The phylogenetic tree was visualized using the FigTree software (v.1.4.4; http://tree.bio.ed.ac.uk/software/figtree).

Based on the alignment of 213 *ppdC* sequences (Table B), three primers pairs were chosen in the most conserved regions, with (i) a size between 18 and 25 nucleotides, (ii) a melting temperature (Tm) between 55 and 62°C, (iii) an absence of predicted hairpin loops, and (iv) an amplification product of 150-300 nucleotides (Table 1).

2.2. PCR primer validation and generation of standard curves from gDNA of pure bacterial strains

To test the amplification specificity of *ppdC* primers, bacterial strains of different *ppdC* phylogenetic clusters were chosen, i.e. *Azospirillum brasilense* Sp7 and Az39, *Azospirillum baldaniorum* Sp245, *Azospirillum lipoferum* CRT1, *Bradyrhizobium* sp. G22, and *Azoarcus* sp. CIB (Figure A.2), as well as *Agrobacterium fabrum* C58 as a negative control. *Azospirillum* strains were grown in modified Nitrogen-free broth (Nfb*; Nfb containing 0.025% of LB; Wisniewski-Dyé et al., 2011), *Bradyrhizobium* sp. G22 in Yeast Extract-Mannitol (YEM) medium, and *Azoarcus* sp. CIB in 1/10 Nutrient Broth (NB). All cultures were incubated under agitation (180 rpm) at 28°C. DNA extraction was performed from an overnight culture of each strain using the method described by Pitcher et al. (1989) for *Azospirillum* strains, or NucleoSpin Tissue kit (Macherey Nagel, Düren, Germany), following manufacturer instructions, for the two other bacteria.

Primer pairs (Table 1) were tested by PCR with 5 µL of buffer 10X, 5 µL of dNTP (2 µM), 2.5 µL of DMSO, 1.5 µL of $MgCl_2$ 50 mM, 1.5 µL of each primer (10 µM), 32.9 µL H_2O, and 0.08 µL of Taq polymerase (Invitrogen, Carlsbad, USA). gDNA was added to obtain a concentration of 40 ng μL^{-1}. DNA was amplified with a 5-min denaturation at 94°C, followed by 35 cycles of 1 min at 94°C, 35 s at 52-62°C, and 35 s at 72°C. A final elongation step of 1 min at 72°C was performed. PCR amplification specificity was determined by checking the presence of a single band of the expected size during gel electrophoresis analysis of the amplification product. Primers 1F*ppdC*/1R*ppdC* and 2F*ppdC*/2R*ppdC* were discarded because of insufficient specificity, and the work was continued with primers 3F*ppdC*/3R*ppdC*.

Standard curves for quantitative PCR were generated using the same six strains. Genomic DNA of each strain was serially diluted ten-fold (in three replicates) to obtain standards from 10^6 to 10 fg DNA mL^{-1}, approximately. Two microliters of each standard dilution were used for qPCR analysis. qPCR assays were conducted using 96-well white microplates, LightCycler 480 SYBR Green I Master mix in a final volume of 20 µL, and a LightCycler 480 (Roche Applied Science, Meylan, France). Reaction conditions included denaturation at 95°C for 10 min, followed by 50 cycles of 15 s denaturation at 95°C, 15 s hybridization at 63°C, and 10 s elongation at 72°C. Amplification specificity was checked by a melting curve analysis of the amplification product, using a fusion program consisting of an initial denaturing step of 5 s at 95°C, an annealing step of 1 min at 65°C, and a denaturing temperature ramp from 65 to 97°C with a rate of 0.11°C s^{-1}. Melting curve calculation and Tm determination were performed using the Tm Calling Analysis module of LightCycler Software v.1.5 (Roche Applied Science). Cycle threshold (Ct) of individual samples was calculated using the second derivative maximum method in the LightCycler Software v.1.5 (Roche Applied Science). The standard curves were obtained by plotting the mean Ct value of the three replicates (per DNA concentration) against log-transformed DNA concentration. Amplification efficiency (E), calculated as $E = 10^{(1/slope)} - 1$, and the Mean Squared Error (MSE) of the standard curve were determined.

2.3. Generation of standard curves from bulk soil inoculated with *ppdC*$^+$ bacterial strains

Ten-fold dilutions of cell suspensions of *A. baldaniorum* Sp245 and *Bradyrhizobium* sp. G22 were prepared and plated onto nutrient agar supplemented with 0.0005% (w/v) bromothymol blue (NAB medium) (for Sp245), or yeast extract mannitol (YEM) agar (for G22). Non-sterile bulk soil samples (500 mg) from LCSA (La Côte St-André, France; Table C.1) field were inoculated with 100 µL of ten-fold dilutions of bacterial cell suspension, from 1.5×10^7 to 1.5×10^2 CFU g^{-1} soil for *A. baldaniorum* Sp245, and 1.8×10^6 to 1.8×10^2 CFU g^{-1} soil for *Bradyrhizobium* sp. G22, or received 100 µL of 0.8% NaCl solution (control). Three samples were prepared for each strain at each inoculum level and for the control. Soil samples were immediately lyophilized (at -50°C for 24 h) and DNA was extracted from the entire samples with FastDNA Spin kit (MP Biomedicals; Irvine, USA), according to manufacturer instructions. For each strain, a standard curve was obtained by plotting the mean Ct value of the three inoculation replicates against log-transformed CFU level. The amplification efficiency and the error were calculated.

2.4. Analysis of indigenous *ppdC*$^+$ bacteria in bulk soil and rhizosphere

DNA was extracted from bulk soil and the rhizosphere of different plants (Table C.1). Briefly, for rhizosphere samples, the root systems were recovered and shaken to remove loosely-adhering soil. Roots and their adhering soil were lyophilised and then rhizosphere soil alone was recovered. DNA was extracted from 500 mg of bulk or rhizosphere soil, as above. DNA samples were analysed by qPCR in triplicate, following the above protocol. The standard curve generated with genomic DNA of *A. baldaniorum* Sp245 was used as the external standard curve for determination of *ppdC* copy number. Results obtained in g μL^{-1} were transformed into numbers of copies g^{-1} soil using the formula [DNA (g) x Avogadro's number (molecules mol^{-1})] / [number of DNA matrix bp in amplified fragments x 660 (g mol^{-1})], based on an average of 660 g mol^{-1} per base pair.

In order to document the bacterial diversity targeted by the *ppdC* primers, the latter were used to prepare Illumina MiSeq sequencing libraries from DNA extracted from LCSA soils (bulk soil and rhizosphere of wheat or tomato), SO4 (rhizosphere of wheat), and C3 (rhizosphere of wheat). PCR was done in duplicate, with *ppdC* primers 3F*ppdC*/3R*ppdC* containing specific Illumina tails (Table C.2), using the HotBioAmp Mix from Biofidal (Lyon, France) supplemented with 0.4X GC-rich enhancer

solution from Biofidal. PCR product purification, amplicon library construction, and Illumina MiSeq sequencing (2 × 300 bp paired-end reads) were performed by Biofidal. A total of 62,286 reads were obtained and demultiplexed. Quality control and sequence analysis were performed using the FROGS pipeline (v. 3.2.1; Escudié et al., 2018). Briefly, the paired-end reads were merged, and sequences without the expected length and/or ambiguous bases were filtered out. Within the FROGS pipeline, the SWARM program (3.0.0; Mahé et al., 2014) was used to cluster the sequences into operational taxonomic units (OTUs) with an aggregation distance of 3. The VSEARCH program was used to remove chimeras (v. 2.15.1; Rognes et al., 2016). Since no *ppdC* database existed for metabarcoding sequencing, we used the 213 sequences already aligned for primer design to develop a database for taxonomic affiliations. The *ppdC* database mentioned above was implemented in FROGS for taxonomic affiliation via the BLASTn method.

The analyses of the obtained sequences were optimized as followed. The 94 non-specific sequences (on the basis that they did not have the expected size and presented 0% alignment with known *ppdC* sequences on NCBI BLASTn tool) identified among the 530 sequences recovered overall (when no size was specified during pre-process treatment of *ppdC* data) were checked for absence of qPCR amplification, by analysing their predicted melting temperature (calculated with uMeltQuartz https://www.dna-utah.org/umelt/quartz/um.php). Indeed, their predicted melting temperatures were 5°C lower than the real melting temperature of *ppdC* sequences, and amplification was not observed during qPCR. Thus, more stringent conditions were used in order to recover only the sequences with the expected size of 197 ± 2 nucleotides.

3. Results

3.1. *ppdC* primers suitable for qPCR

The primers 3F*ppdC*/3R*ppdC* amplified a fragment estimated around 200 bp in size with gel electrophoresis for all six *ppdC*$^+$ strains tested. Real-time PCR conditions were optimized to obtain an amplification efficiency of > 80% and an error below 0.1 with gDNA of all six *ppdC*$^+$ strains (Table C.3). For these strains, amplification was *ppdC*-specific based on melting curve profiles (Tm = 88.5°C, Figure

A.3.A). When tested in non-sterile bulk soil inoculated with *A. baldaniorum* Sp245 or *Bradyrhizobium* sp. G22, amplification efficiencies were above 75% for Sp245 and above 90% for G22, with errors below 0.06 for Sp245 and below 0.03 for G22 (Figure 1). As the non-sterile bulk soil sample showed a Ct-value of 32 (due to indigenous bacteria harbouring the *ppdC* gene), only inoculated samples with a mean Ct-value lower than 32, and thus a higher number of *ppdC* copies than the bulk soil, were taken into account in the calculation of the standard curve. This represented four samples for both strains, *i.e.* dilutions from 10^7 to 10^4 for *A. baldaniorum* Sp24, and dilutions from 10^6 to 10^3 for *Bradyrhizobium* sp. G22.

3.2. Abundance of *ppdC*$^+$ bacteria in bulk soil and rhizosphere

When tested with 6 soils and 10 different plant species (Table C.1), the primers gave melting curve profiles similar to those of pure bacterial strains (Tm = 88.5°C, Figure A.3.B), both for bulk soil and rhizospheric samples, indicating that specific amplification of *ppdC* was achieved from contrasted environmental samples. In bulk soils, the number of *ppdC* copies ranged from 5.47 (in LCSA cropped soil from France) to 7.10 log *ppdC* copies g^{-1} soil (in SO4 from Serbia) (Figure 2). In comparison with bulk soil, values of the same level of magnitude were found in rhizospheric samples, or even higher than 8 log *ppdC* copies g^{-1} (up to 8.55 log *ppdC* copies g^{-1} for basil grown in potting soil). For the three soils where different plant species had been grown (potting soil, LCSA-cropped, and LCSA-meadow), the amplitude for rhizosphere levels was in the order of one log. Therefore, the primer pair 3F*ppdC*/3R*ppdC* allowed to quantify the abundance of *ppdC*$^+$ bacteria in bulk and rhizosphere soils.

3.3. Diversity of *ppdC*$^+$ bacteria in bulk soil and rhizosphere

Primers 3F*ppdC*/3R*ppdC* were used to document the diversity of *ppdC*$^+$ bacteria by Illumina MiSeq metabarcoding in rhizosphere (wheat or tomato) and bulk soil, for soils SO4, C3, and LCSA-cropped. Stringent conditions to recover the sequences with the expected size of 197 ± 2 nucleotides allowed to obtained metabarcoding sequences grouped into 436 *ipdC* OTUs in total (Additional file D.1). Rarefaction curves indicated that the asymptote was reached for all samples (Figure A.4). Five bacterial orders were documented, *i.e.* the *Hyphomicrobiales*, *Rhodospirillales* (*Alphaproteobacteria*), *Burkholderiales*, *Rhodocyclales* (*Betaproteobacteria*), and *Synechococcales* (*Cyanobacteria*), along with unknown

taxonomic groups representing 5 to 10 % of the total *ppdC*$^{+}$ community (Figure 3A). The most abundant *ppdC* orders were the *Hyphomicrobiales* (from 10% for wheat in soil C3 to 60% for wheat in soil LCSA-cropped) and *Rhizobiales* (from 6% for wheat in soil LCSA-cropped to 50% for wheat in soil SO4). Twelve families (or equivalent) were evidenced, i.e. the *Hyphomicrobiaceae*, *Xanthobacteraceae* (*Hyphomicrobiales* order), *Azospirillaceae*, *Rhodospirillaceae* (*Rhodospirillales* order), *Bradyrhizobiaceae* (*Rhizobiales* order), *Comamonadaceae*, *Oxalobacteraceae*, an unclassified *Burkholderiales* group, bacteria related to the genus *Inhella* within the *Sphaerotilus–Leptothrix* group (*Burkholderiales* order), *Rhodocyclaceae*, *Zoogloeaceae (Rhodocyclales* order), and *Leptolyngbyaceae (Synechococcales* order), along with bacteria of unknown family status (representing from 7 to 12% of the total community) (Figure 3B). The most prevalent families were the *Hyphomicrobiaceae* (from 10% for wheat in soil C3 to 60% for wheat in soil LCSA) and the *Bradyrhizobiaceae* (from 7% for wheat in soil LCSA-cropped to 50% for wheat in soil SO4). The phylogenetic tree based on the OTUs from this work and on database sequences showed that our OTUs clustered in 23 clades encompassing a large part of the known diversity of the *ppdC* gene, as only 9 clades did not contain any OTU obtained here (Figure A.5), and encompassed almost all the *ppdC* gene diversity documented so far in soil environments.

4. Discussion

Microbial functioning of the rhizosphere relies on a broad range of microorganisms contributing to plant development, growth, health, or stress tolerance (Lemanceau et al., 2017), hence the importance of better understanding the ecology of the corresponding functional groups. For some of these functional groups, the gene(s) coding for the specific function are highly conserved, which enables the development of molecular tools to monitor them in different soil and plant conditions. It is for example the case for (i) diazotrophic bacteria and archaea, which participate in nitrogen fixation (*nifH* marker) (Bouffaud et al., 2016), and (ii) 1-aminocyclopropane-1-carboxylate deaminase producers, which can diminish ethylene production by roots (*acdS* marker) (Bouffaud et al., 2018; Gebauer et al., 2021; Renoud et al., 2020). However, most plant-beneficial microbial functions remain poorly understood, as the toolbox necessary to

monitor abundance or diversity of the functional group does not exist. This may be due to incomplete knowledge of the genetic basis of certain functions, which means that molecular markers are not yet identified. In addition, a function may be achieved via different genetic pathways, each corresponding to a distinct functional group, making it difficult to assess all organisms that contribute to the function. This is the case for bacterial auxin production.

Here, we focused on the phenylpyruvate decarboxylase pathway and developed primers targeting *ppdC*$^+$ bacteria, because this is the principal IAA synthesis pathway in microbial isolates with phytobeneficial potential (Patten et al., 2012; Spaepen et al., 2007). For a more complete appraisal of IAA producers, further work will be necessary to consider the other relevant functional groups, based on the analysis of genes such as *ipdC* or *iaaM*.

In this work, the first objective was to develop a qPCR method to monitor the abundance of *ppdC*$^+$ bacteria in rhizosphere settings. The analysis of *ppdC* sequences led to the development of the primer pair 3F*ppdC*/3R*ppdC*, which allowed *ppdC* amplification from pure strains inoculated in soil with an efficiency > 80%, a slope between -2.5 and -3.9, and a R^2 > 0.95 (Table C.3). The criteria of Zhang and Fang (2006) were satisfied, with a standard curve in which the cycle threshold is proportional to the log quantity of DNA. Primers proved to be *ppdC* specific and enabled quantification of *ppdC*$^+$ bacteria in different soils and rhizospheres.

The second objective was to determine whether the primers were able to retrieve the *ppdC* allelic diversity documented in bacterial isolates and in metagenomes. It turned out to be the case, based on Illumina MiSeq sequencing data that revealed a large majority of OTUs clustered in the clades present in the corresponding *ppdC* phylogenetic tree (Figure A.3). Most of the clades where no OTUs clustered contained bacteria from sediment, ditch, or marine environment, such as *Sedimenticola selenatireduscens* (Egan et al., 2001), *Aromatoleum bremense* (which can live in anoxic conditions; Rabus et al., 2019; Weiten et al., 2021), and *Pseudoalteromonas ulvae* (Skovhus et al., 2007), or bacteria found in extreme environment e.g. *Thiomonas* sp. (Arsène-Ploetze et al., 2010), all of them unlikely to occur in soil. In addition, one clade of *Bradyrhizobium* did not contain any OTUs, but this genus is mostly adapted to

Fabaceae and may not be favored in the rhizosphere of other plant families. However, it was difficult to go below the order or family level for taxonomic affiliation, as most OTUs blasted with *ppdC* sequences from the database at 85 to 95 % identity levels. There are still some unaffiliated OTUs, indicating that the *ppdC* database does not contain the full diversity of the *ppdC* alleles, and suggesting that a number of microbial strains possessing the *ppdC* gene have not yet been described. Nucleotide BLAST of the corresponding sequences showed they were affiliated with strains of the genera *Thauera, Rhodopseudomonas, Sedimenticola, Azoarcus, Bradyrhizobium*, and *Rhodoferax*. A preliminary assessment of different soil × plant conditions illustrated that both factors are likely to shape *ppdC*$^+$ community diversity in natural conditions, with potentially a stronger effect of the soil type than of the crop species, and these new primers will be useful to document such ecological effects in the rhizosphere.

In conclusion, we report here the first primers targeting microorganisms producing IAA via the phenylpyruvate decarboxylase pathway. These primers will be useful to quantify or describe the diversity of the *ppdC* functional group in the rhizosphere.

Acknowledgements

This work made use of Serre and DTAMB platforms of FR3728 BioEnviS at Université Lyon 1.

References

Ali, B., Sabri, A. N., Ljung, K., and Hasnain, S. 2009. Auxin production by plant associated bacteria: impact on endogenous IAA content and growth of *Triticum aestivum* L. *Lett. Appl. Microbiol.* 48, 542–547. doi:10.1111/j.1472-765X.2009.02565.x.

Arsène-Ploetze, F., Koechler, S., Marchal, M., Coppée, J.-Y., Chandler, M., Bonnefoy, V., et al. 2010. Structure, function, and evolution of the *Thiomonas* spp. genome. *PLOS Genet.* 6, e1000859. doi:10.1371/journal.pgen.1000859.

Bais, H. P., Weir, T. L., Perry, L. G., Gilroy, S., and Vivanco, J. M. 2006. The role of root exudates in rhizosphere interactions with plants and other organisms. *Annu. Rev. Plant Biol*. 57, 233–266. doi:10.1146/annurev.arplant.57.032905.105159.

Bouffaud, M.-L., Renoud, S., Dubost, A., Moënne-Loccoz, Y., and Muller, D. 2018. 1-Aminocyclopropane-1-carboxylate deaminase producers associated to maize and other Poaceae species. *Microbiome* 6, 114. doi:10.1186/s40168-018-0503-7.

Bouffaud, M.-L., Renoud, S., Moënne-Loccoz, Y., and Muller, D. 2016. Is plant evolutionary history impacting recruitment of diazotrophs and *nifH* expression in the rhizosphere? *Sci. Rep.* 6, 1–9. doi:10.1038/srep21690.

Bruto M, Prigent-Combaret C, Muller D, and Moënne-Loccoz Y. 2014. Analysis of genes contributing to plant-beneficial functions in plant growth-promoting rhizobacteria and related *Proteobacteria*. *Sci. Rep.* 4. doi:10.1038/srep06261.

Bulgarelli D, Schlaeppi K, Spaepen S, Ver Loren van Themaat E, Schulze-Lefert P. 2013 Structure and functions of the bacterial microbiota of plants. *Annu. Rev. Plant Biol.* 64, 807-838

Costacurta, A., and Vanderleyden, J. 1995. Synthesis of phytohormones by plant-associated bacteria. *Crit. Rev. Microbiol.* 21, 1–18. doi:10.3109/10408419509113531.

Di, D.-W., Zhang, C., Luo, P., An, C.-W., and Guo, G.-Q. 2015. The biosynthesis of auxin: how many paths truly lead to IAA? *Plant Growth Regul.* 78. doi:10.1007/s10725-015-0103-5.

Edgar, R. C. 2004. MUSCLE: multiple sequence alignment with high accuracy and high throughput. *Nucleic Acids Res.* 32, 1792–1797. doi:10.1093/nar/gkh340.

Egan, S., Holmström, C., and Kjelleberg, S. 2001. *Pseudoalteromonas ulvae* sp. nov., a bacterium with antifouling activities isolated from the surface of a marine alga. *Int. J. Syst. Evol. Microbiol*. 51, 1499–1504. doi:10.1099/00207713-51-4-1499.

Escudié, F., Auer, L., Bernard, M., Mariadassou, M., Cauquil, L., Vidal, K., et al. 2018. FROGS: find, rapidly, OTUs with galaxy solution. *Bioinformatics* 34, 1287–1294. doi:10.1093/bioinformatics/btx791.

Gebauer, L., Bouffaud, M.-L., Ganther, M., Yim, B., Vetterlein, D., Smalla, K., et al. 2021. Soil texture, sampling depth and root hairs shape the structure of ACC deaminase bacterial community composition in maize rhizosphere. *Front Microbiol* 12, 616828. doi:10.3389/fmicb.2021.616828.

Gouy, M., Guindon, S., and Gascuel, O. 2010. SeaView Version 4: A multiplatform graphical user interface for sequence alignment and phylogenetic tree building. *Mol. Biol. Evol*. 27, 221–224. doi:10.1093/molbev/msp259.

Jijón-Moreno, S., Marcos-Jiménez, C., Pedraza, R. O., Ramírez-Mata, A., de Salamone, I. G., Fernández-Scavino, A., et al. 2015. The *ipdC*, *hisC1* and *hisC2* genes involved in indole-3-acetic production used as alternative phylogenetic markers in *Azospirillum brasilense*. *Antonie van Leeuwenhoek* 107, 1501–1517. doi:10.1007/s10482-015-0444-0.

Khalid, A., Arshad, M., and Zahir, Z. A. 2004. Screening plant growth-promoting rhizobacteria for improving growth and yield of wheat. *J. Appl. Microbiol*. 96, 473–480. doi:10.1046/j.1365-2672.2003.02161.x.

Kimura, M. 1980. A simple method for estimating evolutionary rates of base substitutions through comparative studies of nucleotide sequences. *J. Mol. Evol*.16, 111–120. doi:10.1007/BF01731581.

Kochar, M., Upadhay, A., Srivastava, S. 2011. Indole-3-acetic acid biosynthesis in the biocontrol strain Pseudomonas *fluorescens* Psd and plant growth regulation by hormone overexpression. *Res. Microbiol.*162, 426-435. doi: 10.1016/j.resmic.2011.03.006.

Korasick, D. A., Enders, T. A., and Strader, L. C. 2013. Auxin biosynthesis and storage forms. *J. Exp. Bot.* 64, 2541–2555. doi:10.1093/jxb/ert080.

Kunkel, B. N., and Harper, C. P. 2018. The roles of auxin during interactions between bacterial plant pathogens and their hosts. *J. Exp. Bot*. 69, 245–254. doi:10.1093/jxb/erx447.

Lemanceau, P., Blouin, M., Muller, D., and Moënne-Loccoz, Y. 2017. Let the core microbiota be functional. *Trends Plant Sci.* 22, 583–595. doi:10.1016/j.tplants.2017.04.008.

Liu, W. H., Chen, F. F., Wang, C. E., Fu, H. H., Fang, X. Q., Ye, J. R., & Shi, J. Y. 2019. Indole-3-acetic acid in *Burkholderia pyrrocinia* JK-SH007: enzymatic identification of the indole-3-acetamide synthesis pathway. *Front. Microbiol.* 10, 2559. doi: 10.3389/fmicb.2019.02559.

Ljung, K. 2013. Auxin metabolism and homeostasis during plant development. *Development* 140, 943–950. doi:10.1242/dev.086363.

Mahé, F., Rognes, T., Quince, C., Vargas, C. de, and Dunthorn, M. 2014. Swarm: robust and fast clustering method for amplicon-based studies. *PeerJ* 2, e593. doi:10.7717/peerj.593.

Mashiguchi, K., Hisano, H., Takeda-Kamiya, N., Takebayashi, Y., Ariizumi, T., Gao, Y., et al. (2019. *Agrobacterium tumefaciens* enhances biosynthesis of two distinct auxins in the formation of crown galls. *Plant Cell Physiol.* 60, 29–37. doi:10.1093/pcp/pcy182.

Morffy, N., and Strader, L. C. 2020. Old town roads: routes of auxin biosynthesis across kingdoms. *Curr. Opin. Plant Biol.* 55, 21–27. doi:10.1016/j.pbi.2020.02.002.

Narasingarao, P., and Häggblom, Max. M. 2006. *Sedimenticola selenatireducens*, gen. nov., sp. nov., an anaerobic selenate-respiring bacterium isolated from estuarine sediment. *Syst. Appl. Microbiol.* 29, 382–388. doi:10.1016/j.syapm.2005.12.011.

Oberhänsli, T., Défago, G., and Haas, D. 1991. Indole-3-acetic acid (IAA) synthesis in the biocontrol strain CHA0 of *Pseudomonas fluorescens*: role of tryptophan side chain oxidase. *Microbiology* 137, 2273–2279. doi:10.1099/00221287-137-10-2273.

Overvoorde, P., Fukaki, H., and Beeckman, T. 2010. Auxin control of root development. *Cold Spring Harb Perspect Biol* 2, a001537. doi:10.1101/cshperspect.a001537.

Patten, C., Blakney, A., and Coulson, T. 2012. Activity, distribution and function of indole-3-acetic acid biosynthetic pathways in bacteria. *Crit. Rev. Microbiol*. 39. doi:10.3109/1040841X.2012.716819.

Pitcher, D. G., Saunders, N. A., and Owen, R. J. 1989. Rapid extraction of bacterial genomic DNA with guanidium thiocyanate. Lett. Appl. *Microbiol*. 8, 151–156. doi:10.1111/j.1472-765X.1989.tb00262.x.

Prinsen, E., Costacurta, A., Michiels, K., Vanderleyden, J., & Van Onckelen, H. 1993. *Azospirillum brasilense* indole-3-acetic acid biosynthesis: evidence for a non-tryptophan dependent pathway. *Mol. Plant Microbe Int.* 6, 609-609. doi: 10.1094/MPMI-6-609.

Rabus, R., Wöhlbrand, L., Thies, D., Meyer, M., Reinhold-Hurek, B., and Kämpfer, P. 2019. *Aromatoleum* gen. nov., a novel genus accommodating the phylogenetic lineage including *Azoarcus evansii* and related species, and proposal of *Aromatoleum aromaticum* sp. nov., *Aromatoleum petrolei* sp. nov., *Aromatoleum bremense* sp. nov., *Aromatoleum toluolicum* sp. nov. and *Aromatoleum diolicum* sp. nov. Int. J. Syst. Evol. *Microbiol*. 69, 982–997. doi:10.1099/ijsem.0.003244.

Renoud, S., Bouffaud, M.-L., Dubost, A., Prigent-Combaret, C., Legendre, L., Moënne-Loccoz, Y., et al. 2020. Co-occurrence of rhizobacteria with nitrogen fixation and/or 1-aminocyclopropane-1-carboxylate deamination abilities in the maize rhizosphere. *FEMS Microbiol. Ecol.* 96. doi:10.1093/femsec/fiaa062.

Roesch, L. F. W., de Quadros, P. D., Camargo, F. A. O., and Triplett, E. W. 2007. Screening of diazotrophic bacteria *Azopirillum* spp. for nitrogen fixation and auxin production in multiple field sites in southern Brazil. *World J. Microbiol. Biotechnol.* 23, 1377–1383. doi:10.1007/s11274-007-9376-9.

Rognes, T., Flouri, T., Nichols, B., Quince, C., and Mahé, F. 2016. VSEARCH: a versatile open source tool for metagenomics. *PeerJ* 4, e2584. doi:10.7717/peerj.2584.

Scarpella, E., Barkoulas, M., and Tsiantis, M. 2010. Control of leaf and vein development by auxin. *Cold Spring Harb Perspect Biol* 2, a001511. doi:10.1101/cshperspect.a001511.

Schütz, A., Golbik, R., Tittmann, K., Svergun, D. I., Koch, M. H. J., Hübner, G., et al. 2003. Studies on structure–function relationships of indolepyruvate decarboxylase from *Enterobacter cloacae,* a key enzyme of the indole acetic acid pathway. *Eur. J. Biochem*. 270, 2322–2331. doi:10.1046/j.1432-1033.2003.03602.x.

Skovhus, T. L., Holmström, C., Kjelleberg, S., and Dahllöf, I. 2007. Molecular investigation of the distribution, abundance and diversity of the genus *Pseudoalteromonas* in marine samples. *FEMS Microbiol*. Ecol. 61, 348–361. doi:10.1111/j.1574-6941.2007.00339.x.

Spaepen, S., Vanderleyden, J., and Remans, R. 2007. Indole-3-acetic acid in microbial and microorganism-plant signaling. *FEMS Microbiol. Rev*. 31, 425–448. doi:10.1111/j.1574-6976.2007.00072.x.

Tsavkelova, E. A., Cherdyntseva, T. A., and Netrusov, A. I. 2005. Auxin production by bacteria associated with orchid roots. *Microbiology* 74, 46–53. doi:10.1007/s11021-005-0027-6.

Vacheron, J., Desbrosses, G., Bouffaud, M.-L., Touraine, B., Moënne-Loccoz, Y., Muller, D., et al. 2013. Plant growth-promoting rhizobacteria and root system functioning. *Front. Plant Sci.* 4. doi:10.3389/fpls.2013.00356.

Weiten, A., Kalvelage, K., Becker, P., Reinhardt, R., Hurek, T., Reinhold-Hurek, B., et al. 2021. Complete genomes of the anaerobic degradation specialists *Aromatoleum petrolei* ToN1T and *Aromatoleum bremense* PbN1T. *MIP* 31, 16–35. doi:10.1159/000513167.

Wisniewski-Dyé, F., Borziak, K., Khalsa-Moyers, G., Alexandre, G., Sukharnikov, L. O., Wuichet, K., et al. 2011. *Azospirillum* genomes reveal transition of bacteria from aquatic to terrestrial environments. *PLOS Genetics* 7, e1002430. doi:10.1371/journal.pgen.1002430.

Zimmer, W., Wesche, M., Timmermans, L. 1998. Identification and isolation of the indole-3-pyruvate decarboxylase gene from *Azospirillum brasilense* sp7: sequencing and functional analysis of the gene locus. Cur. Microbiol. 36, 327-331. doi: 10.1007/s002849900317

Zhang, T., and Fang, H. H. P. 2006. Applications of real-time polymerase chain reaction for quantification of microorganisms in environmental samples. *Appl. Microbiol. Biotechnol.* 70, 281–289. doi:10.1007/s00253-006-0333-6.

Zhang, P., Jin, T., Kumar Sahu, S., Xu, J., Shi, Q., Liu, H., & Wang, Y. 2019. The distribution of tryptophan-dependent indole-3-acetic acid synthesis pathways in bacteria unraveled by large-scale genomic analysis. *Molecules* 24, 1411. doi: 10.3390/molecules24071411.

Zhao, Y. 2014. Auxin Biosynthesis. *Arabidopsis Book* 12. doi:10.1199/tab.0173.

Legends

Figure 1. qPCR standard curves for *Azospirillum baldaniorum* Sp245 and *Bradyrhizobium* sp. G22 inoculated in non-sterile LCSA-meadow bulk soil. Strains were inoculated at different CFU levels. Mean Ct values from three replicates are shown.

Figure 2. qPCR quantification of *ppdC*$^+$ bacteria in bulk soil and rhizosphere. LCSA-c, cropped LCSA soil ; LCSA-m, meadow LCSA soil. Bulk soils and plants are listed in Table C.1.

Figure 3. Relative abundance of *ppdC*$^+$ bacterial orders (A) and families (B) associated with rhizosphere and bulk soil. Bulk soils and plants are listed in Table C.1. In A, the *Alphaproteobacteria* are shown in purple colors, the *Betaproteobacteria* in yellow colours, the *Cyanobacteria* in green, and unknown taxa in grey. In B, the *Hyphomicrobiales* are shown in purple colours, the *Rhodospirillales* in dark green colours, the *Rhizobiales* in yellow, the *Burkholderiales* in pink colours, the *Rhodocyclales* in blue colours, the *Synechococcales* in light green, and the bacteria of unknown family status in grey.

Figure 1.

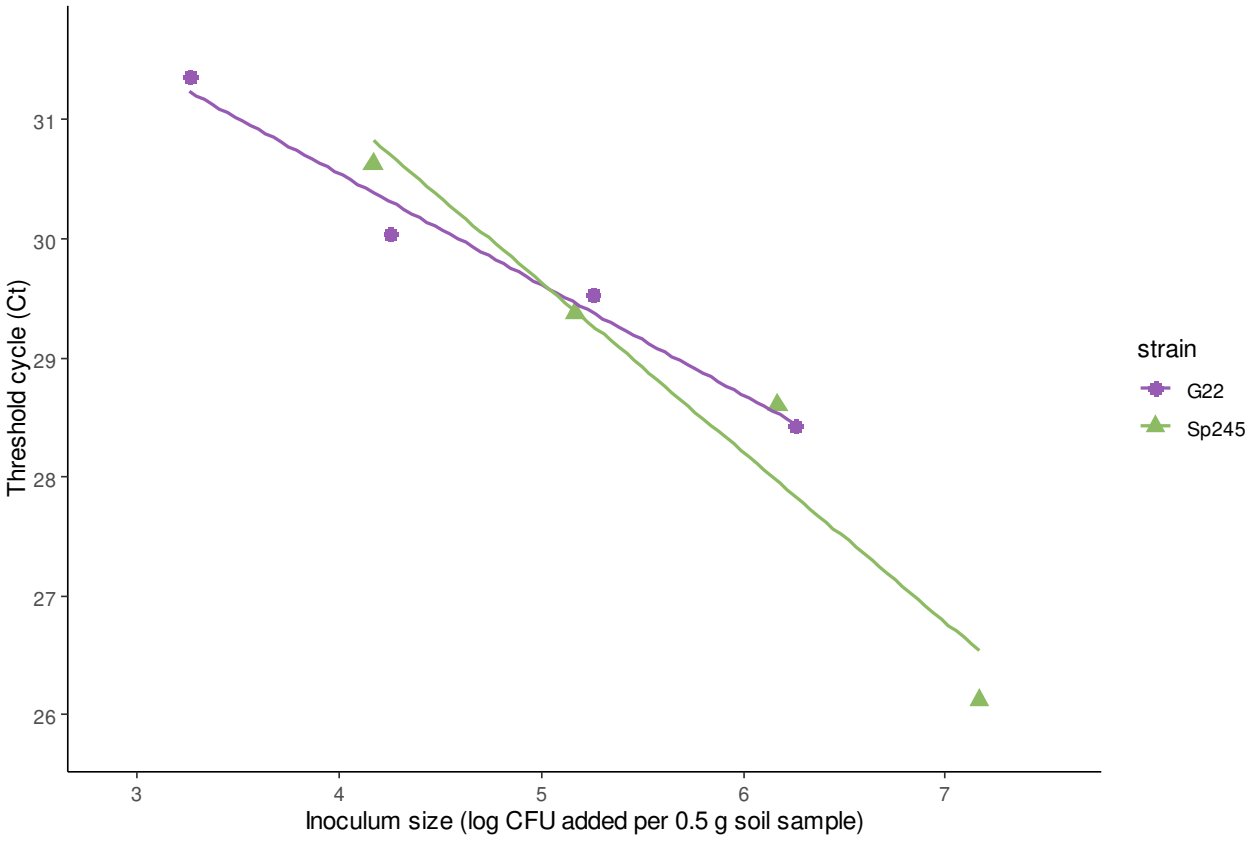
Threshold cycle (Ct)
31
30
29
28
27
26
3
4
5
6
7
Inoculum size (log CFU added per 0.5 g soil sample)
strain
G22
Sp245

Figure 2.

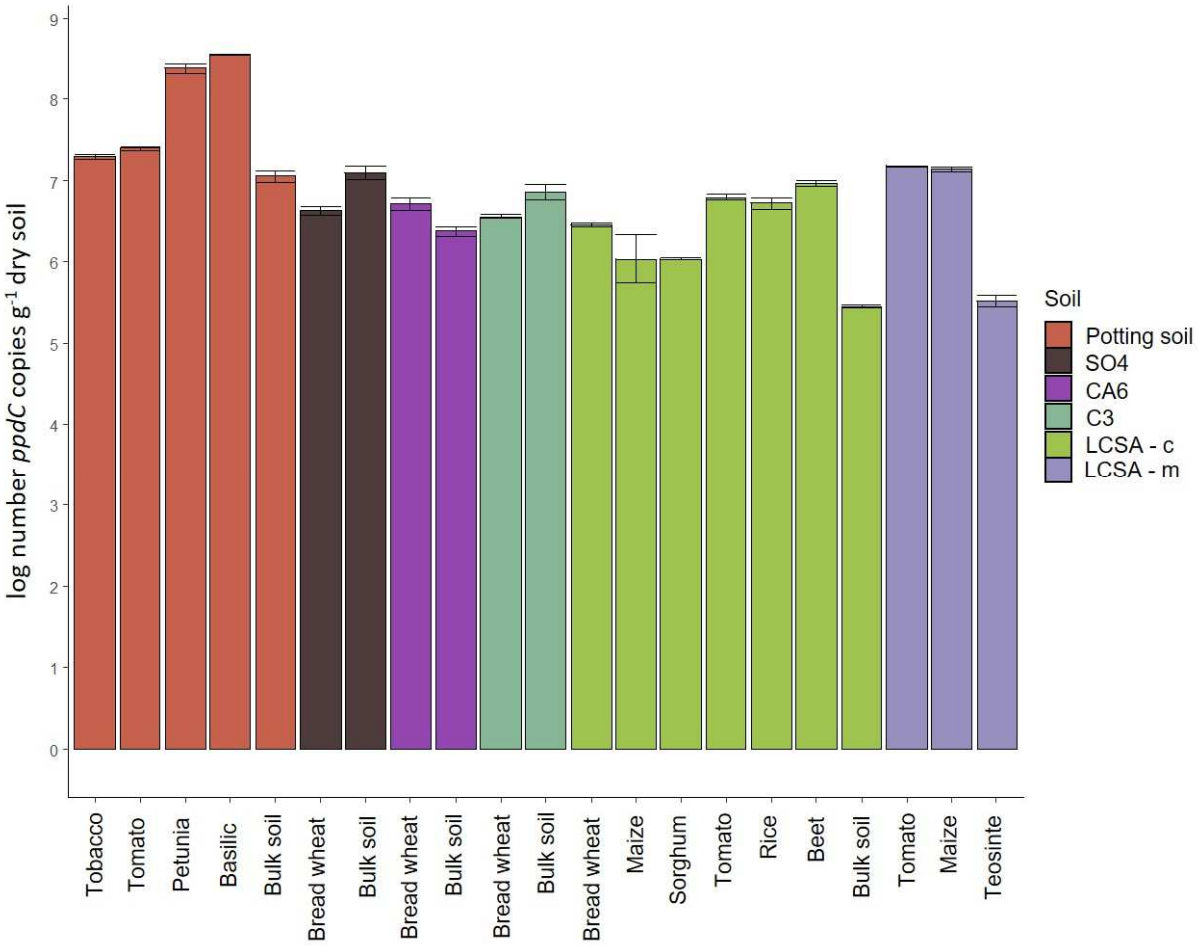
log number ppdC copies g-1 dry soil
0
1
2
3
4
5
6
7
8
9
Tobacco
Tomato
Petunia
Basilic
Bulk soil
Bread wheat
Bulk soil
Bread wheat
Bulk soil
Bread wheat
Bulk soil
Bread wheat
Maize
Sorghum
Tomato
Rice
Beet
Bulk soil
Tomato
Maize
Teosinte
Soil
Potting soil
SO4
CA6
C3
LCSA - c
LCSA - m

Figure 3.

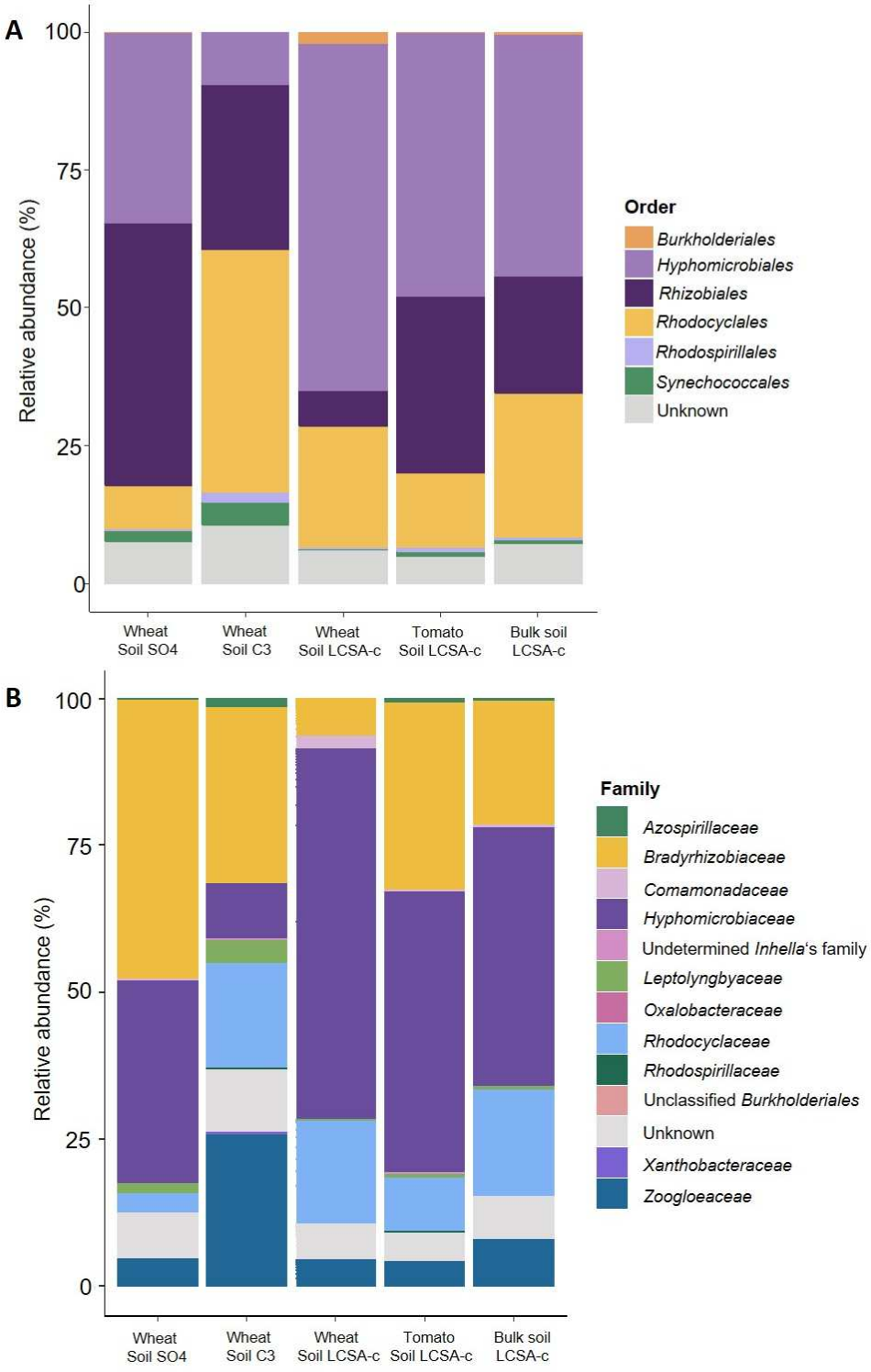
A
100
75
50
25
0
Relative abundance (%)
Wheat Soil SO4
Wheat Soil C3
Wheat Soil LCSA-c
Tomato Soil LCSA-c
Bulk soil LCSA-c
Order
Burkholderiales
Hyphomicrobiales
Rhizobiales
Rhodocyclales
Rhodospirillales
Synechococcales
Unknown
B
100
75
50
25
0
Relative abundance (%)
Wheat Soil SO4
Wheat Soil C3
Wheat Soil LCSA-c
Tomato Soil LCSA-c
Bulk soil LCSA-c
Family
Azospirillaceae
Bradyrhizobiaceae
Comamonadaceae
Hyphomicrobiaceae
Undetermined Inhella's family
Leptolyngbyaceae
Oxalobacteraceae
Rhodocyclaceae
Rhodospirillaceae
Unclassified Burkholderiales
Unknown
Xanthobacteraceae
Zoogloeaceae

Table 1. Primer pairs designed for *ppdC* amplification

Primers	Sequence	Amplicon size
1F*ppdC*	5’ AGGTNTTCAAGGAGATCACC 3’	277 pb
1R*ppdC*	5’ ACGCKGACCATCAGCACC 3’	
2F*ppdC*	5’ CCGGTGGTSACCACCTTC 3’	254 pb
2R*ppdC*	5’ GBGTAGGTGTGATAGCCCA 3’	
3F*ppdC*	5’ GGCGACTGCCTGTTCACC 3’	236 pb
3R*ppdC*	5’ CCAGCTGGCGTTGTTGAAC 3’	